

The dual roles of RPE65 S-palmitoylation in membrane association and visual cycle function

Sheetal Uppal¹, Tingting Liu^{1,2}, Eugenia Poliakov¹, Susan Gentleman¹, and T. Michael Redmond^{1*}

¹Laboratory of Retinal Cell and Molecular Biology, National Eye Institute, National Institutes of Health, Bethesda, MD 20892, United States

²Present address: Department of Transfusion, The Affiliated Drum Tower Hospital of Nanjing University Medical School, Nanjing 210008, P.R. China

*Address correspondence to: redmondtd@helix.nih.gov; Tel.: 301-496-0439; Fax: 301-402-1883.

Supplemental Figure Legends

Figure S1. **Co-existence of palmitoylated and non-palmitoylated populations of RPE65.** Acyl-RAC analysis of RPE65 showed that a major population of RPE65 did not pull down with thiopropyl-sepharose beads (unbound fraction). The palmitoylation status of this unbound RPE65 was checked by twice sequentially re-incubating unbound fraction (unbound fraction 1 and 2) with fresh beads, followed by immunoblot analysis using anti-RPE65 antibody. This showed that there was no pulldown of this population of RPE65, confirming its lack of palmitoylation.

Figure S2. **Amino acid sequence alignment of RPE65 from different species.** Sequence alignment shows the position of non-conserved (in blue color) and conserved (in red color) cysteine residues among different species. Note that only in one of three paralogs in teleost fishes and in hagfish RPE65 is C146 not completely conserved. There are 12 cysteine residues in bovine RPE65. Dog RPE65 has 11 cysteine residues, with substitution of the non-conserved cysteine 396 (present in human and bovine RPE65s) to an arginine residue.

Figure S3. **Structural view of surface exposed cysteine residues.** Surface view of dog RPE65 structure was visualized and generated using PyMol software. Close inspection of the cysteine residues on the three-dimensional structure of RPE65 revealed five cysteines (C112, C169, C195, C278 and C448, as shown in red color; highlighted in circle) that have their thiol groups facing to the solvent. The iron (Fe) atom in the center of the RPE65 structure is represented by orange color.

Figure S4. **Identification of cysteine residues involved in RPE65 palmitoylation.** HEK293F cells were transfected with cysteine mutants of RPE65 to determine the residues that undergo palmitoylation. Cell lysate was prepared (as described in Materials and Methods section) and used for ABE and acyl-RAC analysis. (A) ABE result of cysteine 112, 146 and 195 mutants compared to wild type RPE65. (B) Acyl-RAC results for both alanine and serine substituted mutants of cysteine residues other than C112, C146 and C195 showed a protein band in the HAM-treated samples and so did not affect palmitoylation of RPE65. (C) Serine substituted C112, C146 and C195 residues showed reduced or no RPE65 band in the HAM-treated samples, and thus are involved in RPE65 palmitoylation. Samples were treated with 0.5 M hydroxylamine (HAM; indicated as "+") or 0.5 M NaCl (indicated as "-"), respectively. Results were calculated as mean \pm S.D. from three independent experiments. *P<0.005, **P<0.05, unpaired student's t-test.

Figure S5. **Mass spectrometric analyses of control and hydroxylamine-treated samples for rhodopsin and CRALBP.** Comparison of relative abundance of NEM- and 4-VP modified peptides in the control and HAM-treated samples for rhodopsin (A) and CRALBP (B). N-ethyl maleimide (NEM) and 4-vinyl pyridine (4-VP) modification represents the non-palmitoylation and palmitoylation of cysteine residues, respectively. We identified the peptide containing 4-VP modifications of cysteines 322 and 323 from the bovine rhodopsin sample. In the case of CRALBP, only NEM-modified peptides were detected, indicating lack of palmitoylation. The square box represents the technical replicates of the sample) and the line represent the comparative behavior of the peptide ion of interest in the – HAM and + HAM samples.

Figure S6. **MS-coupled acyl-labeling of bovine microsome RPE using different MS instruments, Synapt G2-Si HDMS, AB Sciex 6600 w/SelexION.** Rhodopsin and CRALBP were used as positive and negative control. NEM- and 4VP-modified cysteine indicates non-palmitoylation and palmitoylation of cysteine residue, respectively. The ratio of modified peptide shown was relatively high in hydroxylamine-treated samples compared to untreated samples.

Figure S7. **Immunoblot analysis of proteins in HEK293F-based heterologous visual cycle system.** HEK293F cells transfected with pViro2/RPE65+CRALBP and pViro3/LRAT or LRAT^{C161S} mutant+RDH5 plasmids were analysed by western blotting for RPE65, CRALBP, LRAT, and RDH5.

Figure S8. **Expression profiles of wild type and C112, C146 and C195 mutant RPE65 protein.** HEK293F cells were transfected with pVITRO2/RPE65 wild type or cysteine mutants +CRALBP and ~10 μ g of total protein were analysed by western blotting for expression analysis. The same samples were then subjected to subcellular fractionation shown in Figure 6D.

Figure S9. **Presence of C112 mutant protein in lysosomal fraction.** HEK293F cells transfected with pVITRO2/RPE65 wild type or C112 mutants +CRALBP were subjected to lysosomal extraction kit (Sigma) and then the lysosomal fractions were analysed by western blotting for RPE65 and cathepsin D (lysosomal marker protein).

Figure S10. **Enlarged view of the catalytic core of RPE65 showing rotamer variability of cysteine 195.** Structural representation of RPE65 (PDB ID: 4RSC; chain A) in complex with the non-retinoid inhibitor emixustat and palmitate. Iron (Fe) atom in the center is represented in orange color. Residues C146 and C195 are denoted as stick figures on the cartoon to mark the orientation of the thiol group. The thiol group (marked with arrows) of C195 exists in two different conformations Asterisks (*) represent the location of the unresolved loop (residues G196-S201) in the ligand bound RPE65.

Figure S11. **Surface view of crystal structure of RPE65.** A, RPE65 structure showing three hydrophobic regions. The region consisting of aa109-125 is generated by the ITASSER server (shown in yellow). B, hydrophobic surface view of RPE65 as predicted by PyMOL server. Red color indicates the hydrophobic surface.

Figure S12. **Enlarged view of the catalytic core of RPE65 showing the approximate distance of 8 Å between the bound palmitate and C146 thiol atom.** The dashed yellow line represent the measured distance between the bound palmitate and C146-thiol atom in the palmitate-bound crystal structure of RPE65 (PDB ID: 4RSC).

Figure S13. **Original western blot panels with gel markers for Figures 1A, 1C, 2B, 5A, 5B, 5C, 6, S1, S2, S3, S6A, S6C, S8, and S9.** Complete scanned gels for western blots shown. Red dashed line identifies cropped region shown in respective figure.

Figure S1

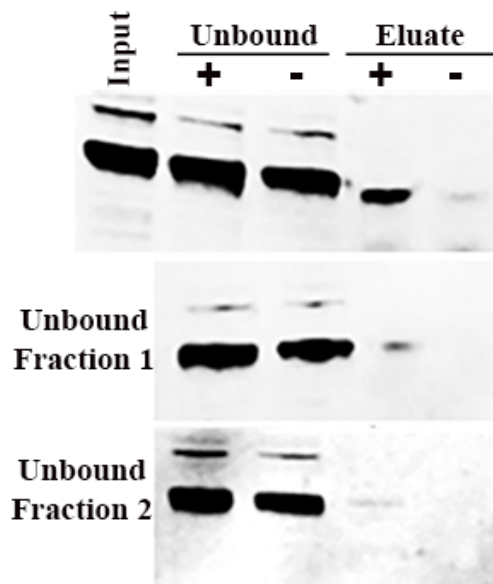


Figure S2

```

BOVINE 1 MSSQVEHPAGGYKKLFETVEELSSPLTAHVTRGRIPLWLTGSLLR45CGPLFEVGGSEPFYHLFDGQALLHKFDFKEGHVTYHRRFIRTDAYVRAMTEKRIVI 100
HUMAN 1 I 100
DOG 1 100
MOUSE 1 I I 100
CHICK 1 Y V T R A V 100
SALAM 1 TNR D ST VA V Q V S A Q E G I T 100
ZEBRFI 1 V RF I A NE T SFIK L A A M SN Q F K VK I V 100
LAMPRI 1 ATC K TA Y AQ VKT MPTQ Q S S M L E L EISN A AC LK T N A 100
HAGFI 1 M-YCF S A Y TENSVPPTIQ H D N L C L M IRK TS LL S 99
106 112 146 169 195
BOVINE 101 TEFGTC106AFPPD112CKNIFSRFFSYFRGVEVTDNALVNIYPVGGEDYYA146CTETNFITKVNPELETIKQVDL169CONYVSVNGATAHPHIENDGTVINIGN195CFGKNF 200
HUMAN 101 V I 200
DOG 101 I 200
MOUSE 101 K I S 200
CHICK 101 Y Y K V I D K V 200
SALAM 101 F L Q L V Y I V K I V H 200
ZEBRFI 101 Y K C V I F V Y VD L K M NI V R M GA 200
LAMPRI 101 V Y QKI I F S I VAK K I I R GL 200
HAGFI 101 F Y L I T V I SF S YV D LGK D CVI V A I RM 199
231 278
BOVINE 201 SIANYIVKIPPLQADKEDPISKSEIVVQFF231CSDRFKPSYVHSGFLTPNYIVFVETPVKINLFKFLSSWSLWGANMDC278FESNETMGVWLHIADKKRKYI 300
HUMAN 201 L 300
DOG 201 L 300
MOUSE 201 TV I K N V S V R F 300
CHICK 201 L IR MN V L V E KGRLL 300
SALAM 201 AF N AKV E Q I H M V E HTGE L 300
ZEBRFI 201 L R T K S E KV SAE M E F Q L A IR S D EK T I R HPGE 300
LAMPRI 201 F I LK VN LN MSVA L E M E F Q W A GPR T HH V V R GE 300
HAGFI 201 NEF IR M D LK LKV TS RE KSE F Q W A GPR S D IV T I V HSGEVL 299
329330 396
BOVINE 301 NNKYRTSPFNLFHHINTYEDHEFLIVDL329330CKWGFEFVYNYLYLANLRENWEEVKKNARKAPQEVRRYVLPNLIDKADTGKNLVTLPTNTATALL396CSDET 400
HUMAN 301 NG 400
DOG 301 S N S T V R H T R 400
MOUSE 301 R M A T V R H T R 400
CHICK 301 I A F T A D Q E A R Y T R 400
SALAM 301 I A H R S E P D H V N Y V R 400
ZEBRFI 301 DY F AMG C S IVF A W A R MI I DPFREEQ IS Y TMRA G 400
LAMPRI 301 DIRF AAA I F KEGHIVM V I M L R Y I F EEEY R GD T RN G 400
HAGFI 301 PTT S I EDGQIVA Y S DK NLKN448CALE HLEE EF RVQH T RH G 399
448
BOVINE 401 IWLEPEVFLSGPRAQAFEPQIN448YQYGGKPYTYAYGLGLNHFPDR448CKLVNKTKETVWVQEPDSYPSEPIFVSHPDAL448EDDGVVLSVVSPG-AGQKP 500
HUMAN 401 C 500
DOG 401 500
MOUSE 401 F K I M Q 500
CHICK 401 V I H K T V I I S P 500
SALAM 401 K H D V S T Q I I E 500
ZEBRFI 401 RMVN N I R L QT GVD ILMTI - R 499
LAMPRI 401 R E NN RD F KIY H I GT IAR QD L TT P RT 501
HAGFI 400 V D KRCN N KIY QML HT T IAR GTE LVTS A S S 499
BOVINE 501 AYLLILNARDLSEVARAEVEINI533PVTFHGLFKKS--- 533
HUMAN 501 533
DOG 501 533
MOUSE 501 V I T R 533
CHICK 501 M V RA 533
SALAM 501 F M I DS M A 533
ZEBRFI 500 T C I LT MY P- 531
LAMPRI 502 F T DV S M KE SKH 536
HAGFI 500 F L D R T L DR M T- 532

```

Figure S3

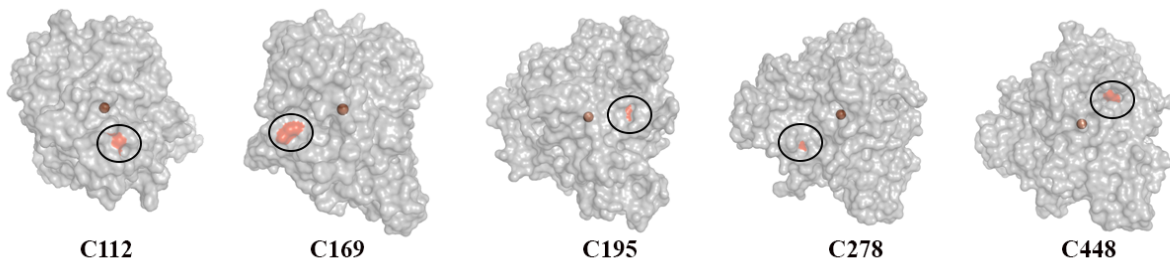


Figure S4

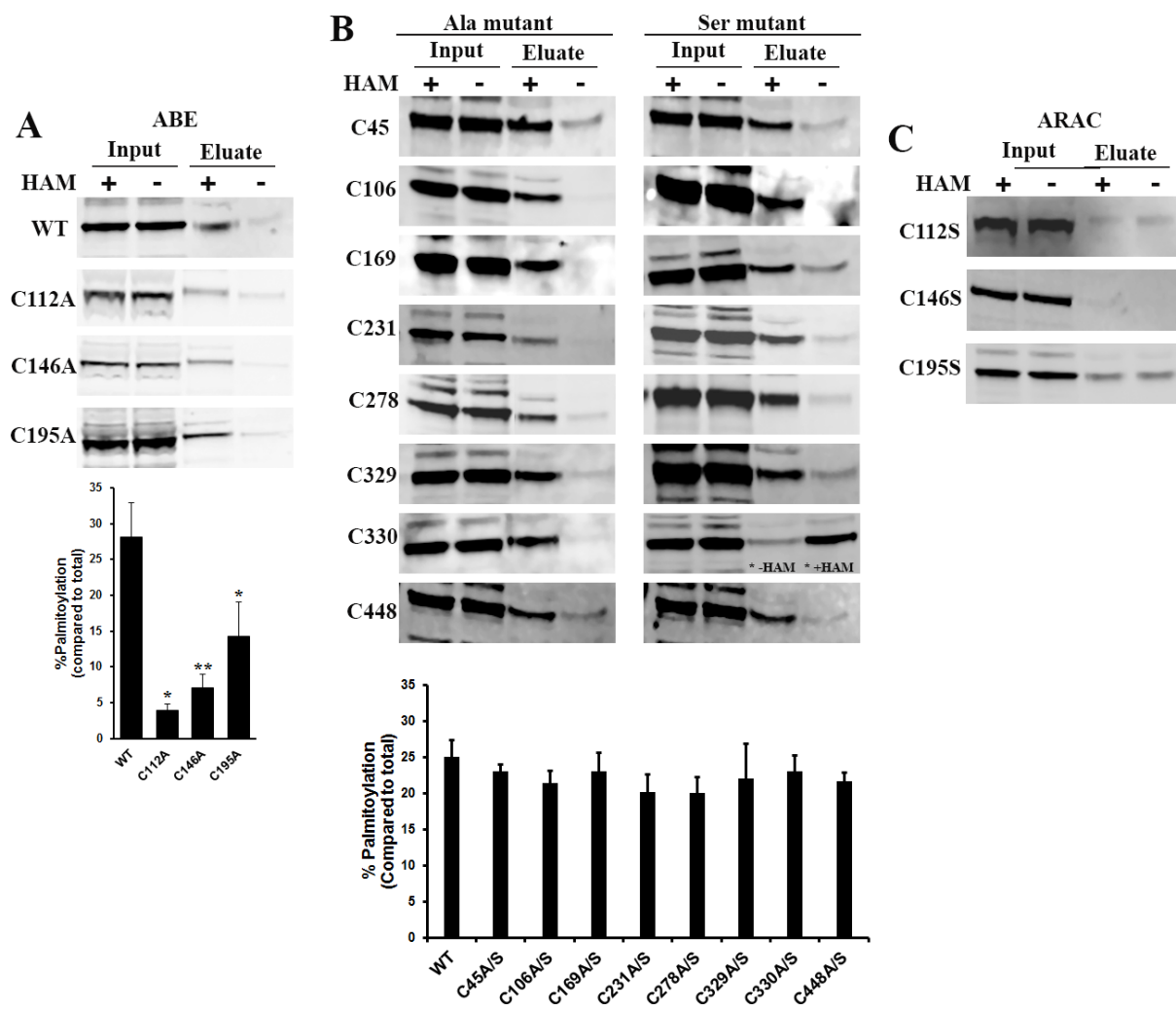
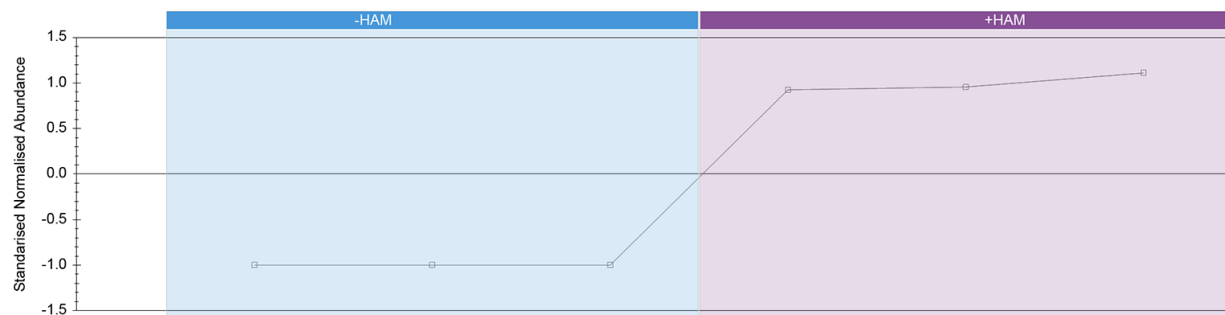


Figure S5

A Rhodopsin: QFRN³¹⁶C_{NEM}MVTTL³²²C_{4-VP}³²³C_{4-VP}GKNPLGDDEASTTVSK



B CRALBP: DHGPVFGP³⁸C_{NEM}SQLPR and ¹³⁸C_{NEM}TVEAGYPGVLSTR

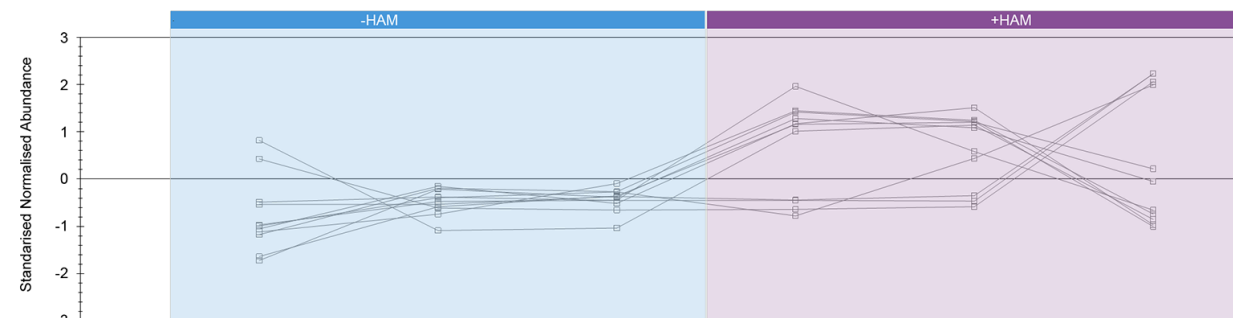


Figure S6

Rhodopsin (palmitoylated protein)		
Peptides	Synapt G2-Si HDMS ^E	AB Sciex6600 w/SelexION
K.QFRNCMVTTL ₃₂₂ C ₃₂₃ CG KNPLGDDEASTTVSK.T	₃₂₂ C: 4VP ₃₂₃ C: 4VP	₃₂₂ C: 4VP ₃₂₃ C: 4VP
CRALBP (non-palmitoylated protein)		
Peptides	Synapt G2-Si HDMS ^E	AB Sciex6600 w/SelexION
K.DHGPFVFGP ₃₈ CSQLPR.H R. ₁₃₈ CTVEAGYPGVLSTR.D	₃₈ C: NEM ₁₃₈ C: NEM	₃₈ C: NEM ₁₃₈ C: NEM
RPE65		
Peptides	Synapt G2-Si HDMS ^E	AB Sciex6600 w/SelexION
R.IVITEFGT ₁₀₆ CAFPDP ₁₁₂ CK.N R.GVEVTDNALVNIYPVGEDY YA ₁₄₆ CTETNFITK.V K.QVDL ₁₆₉ CNYVSVNGATAHP HIENDGTVYNIGN ₁₉₅ CFG.K	₁₀₆ C: NEM ₁₁₂ C: NEM; 4VP ₁₄₆ C: 4VP ₁₆₉ C: NEM ₁₉₅ C: NEM	₁₀₆ C: NEM ₁₁₂ C: 4VP ₁₄₆ C: NEM ₁₆₉ C: NEM ₁₉₅ C: NEM

Figure S7

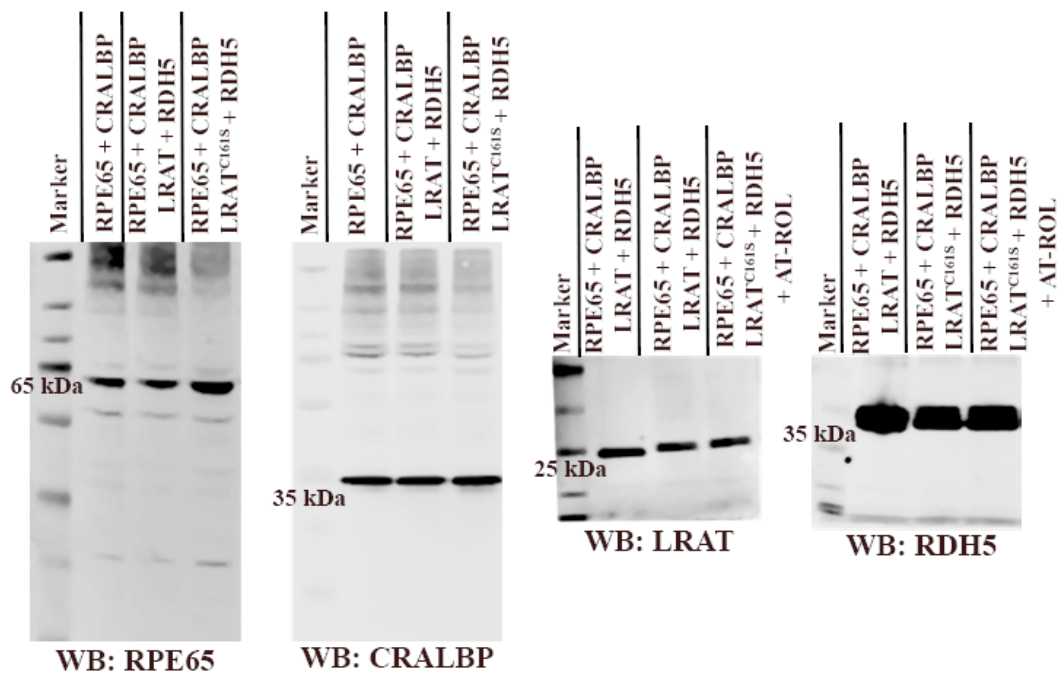


Figure S8

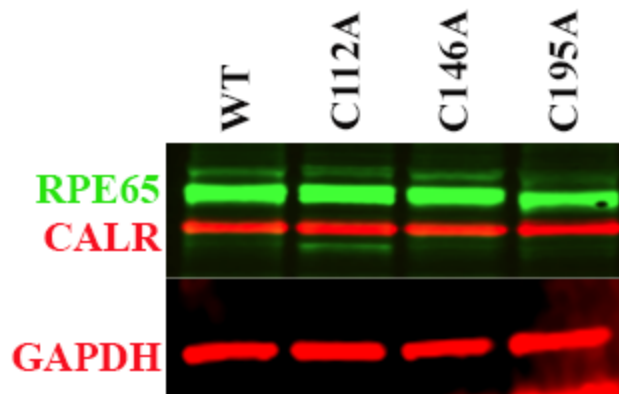


Figure S9

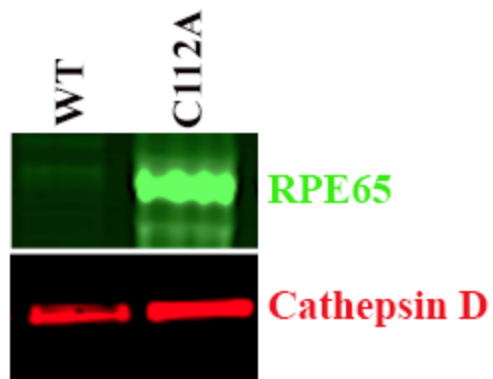


Figure S10

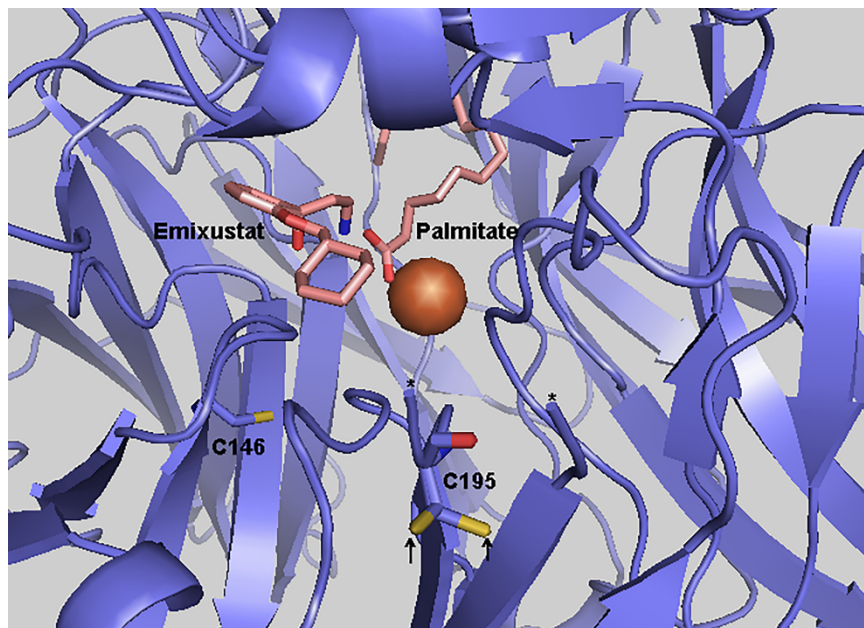


Figure S11

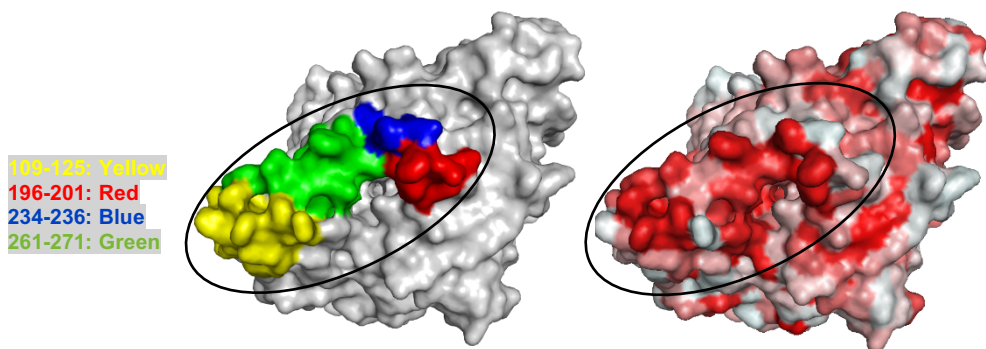


Figure S12

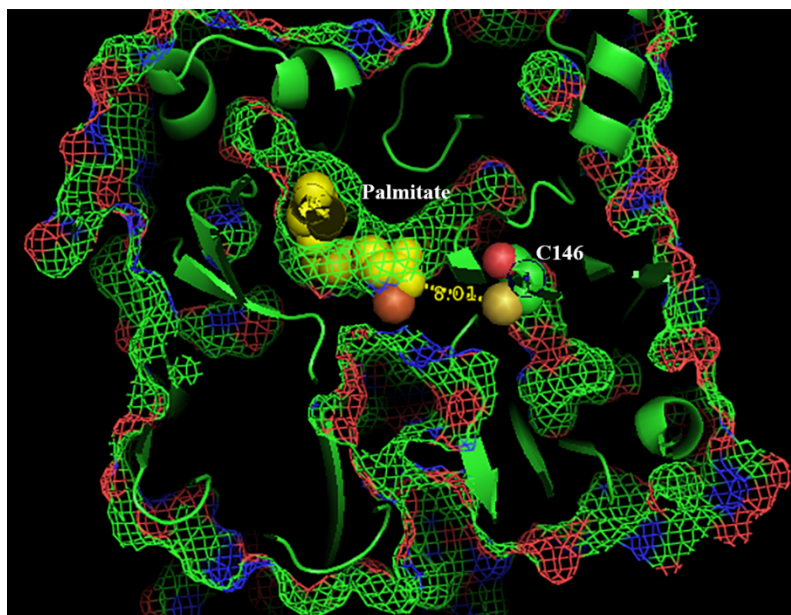


Figure S13

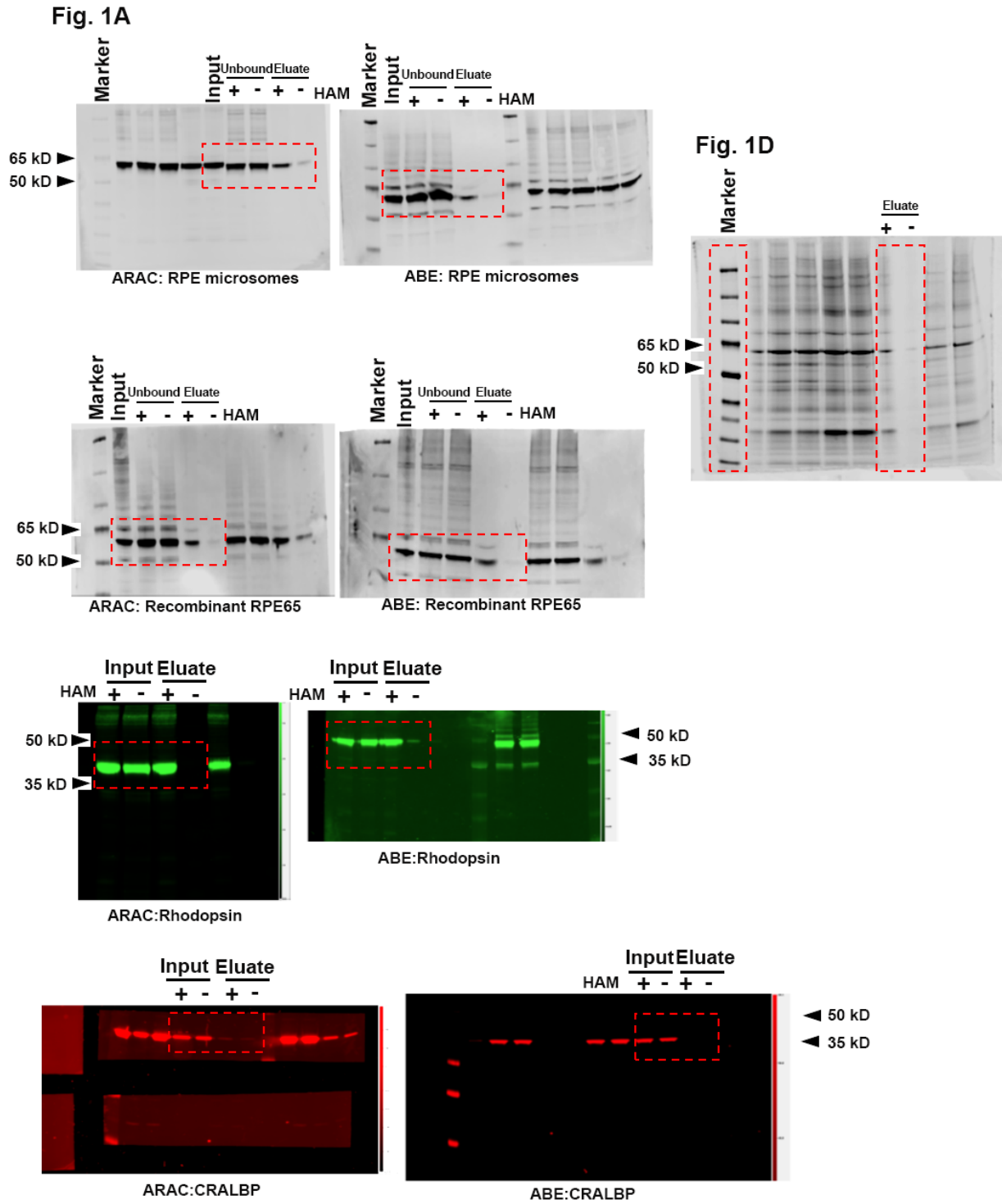
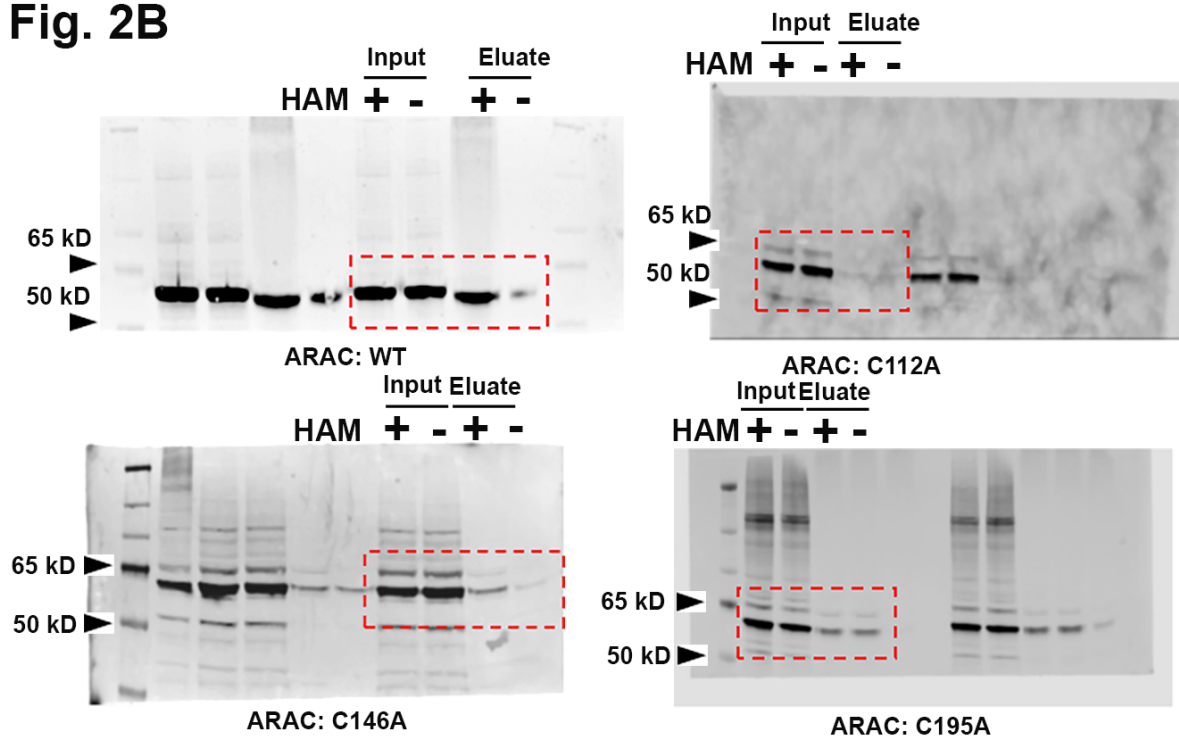
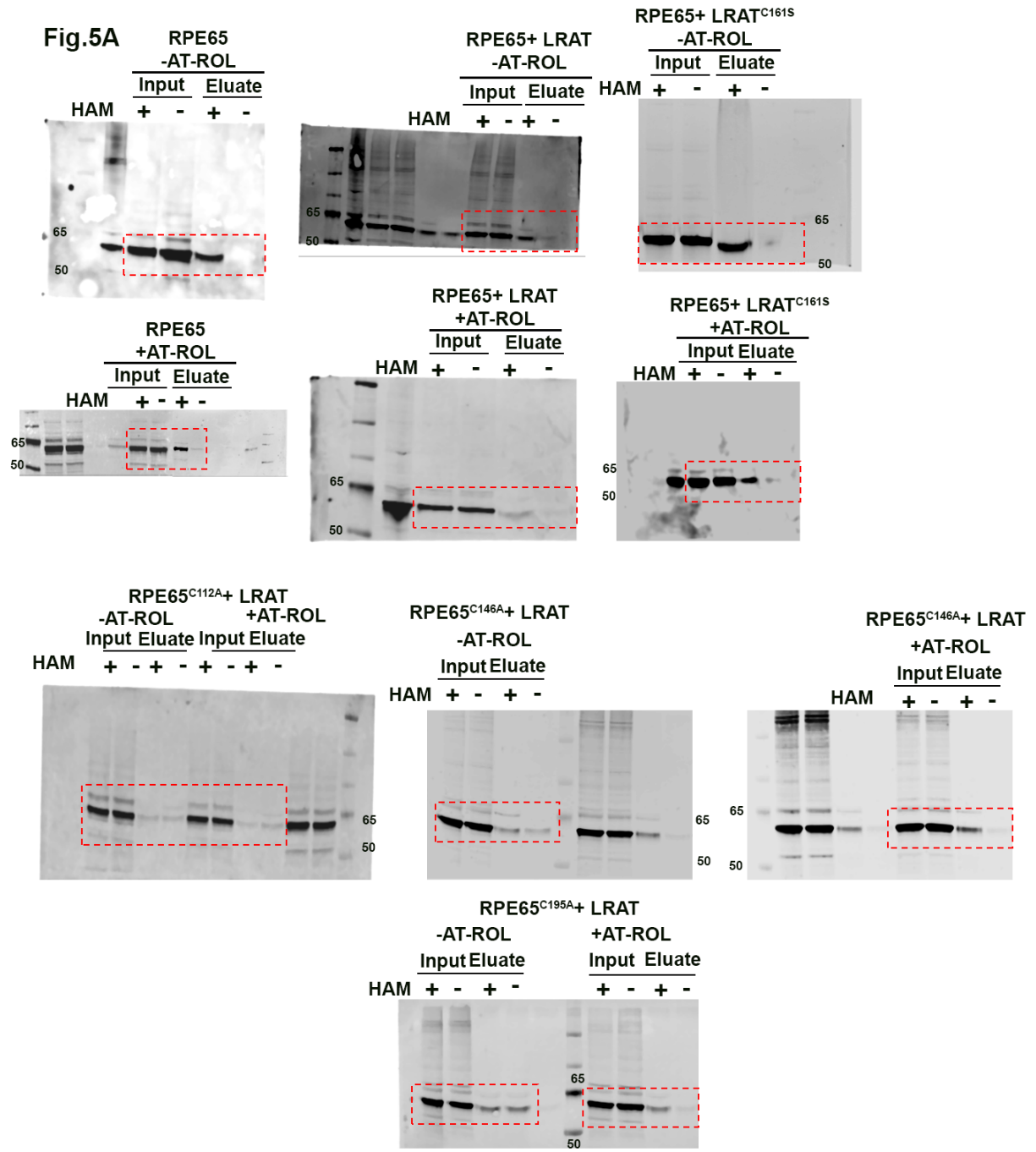


Fig. 2B





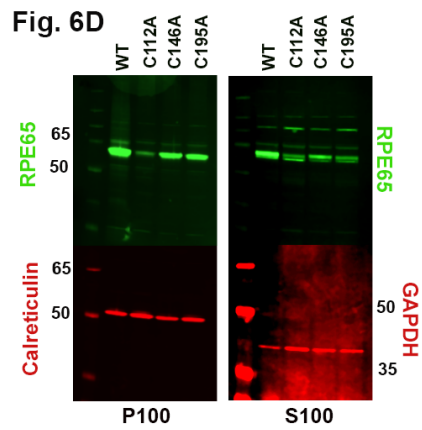
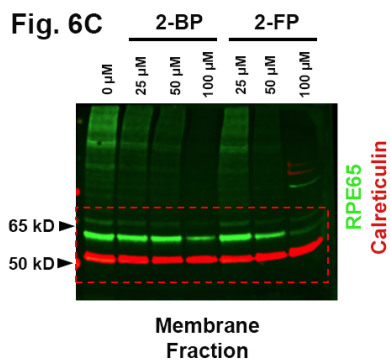
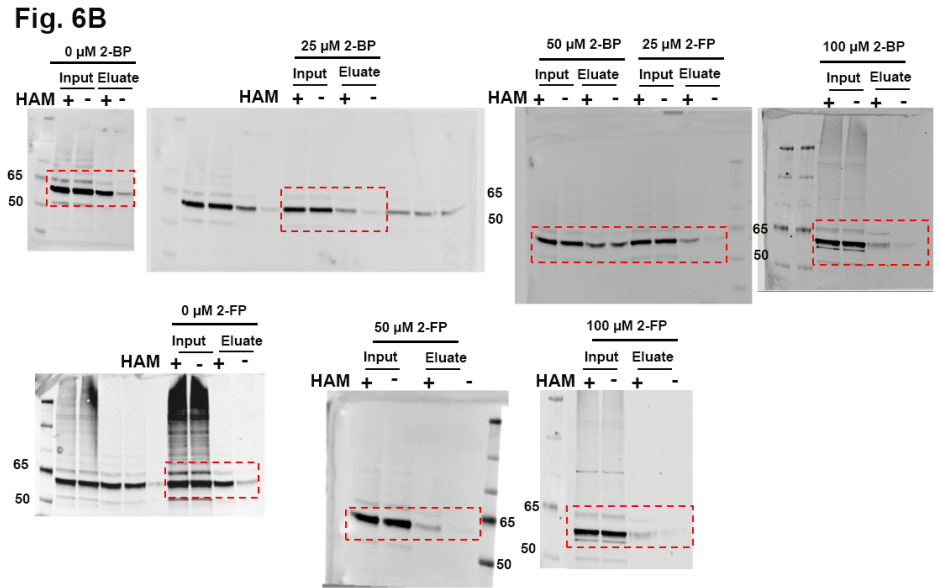
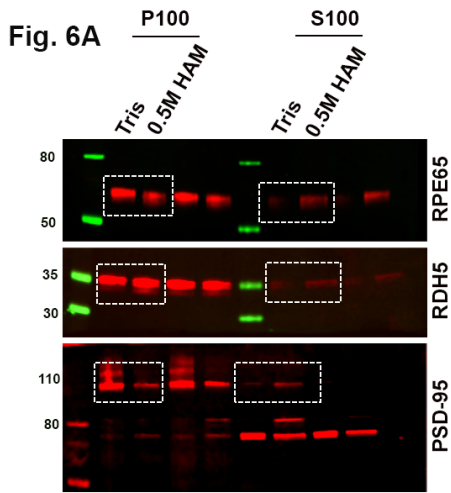


Fig. S1

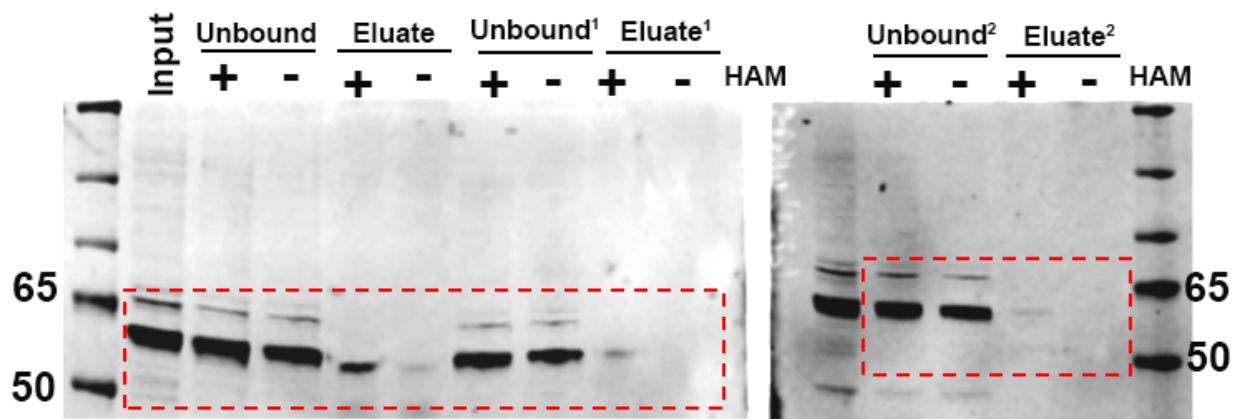


Fig. S4A

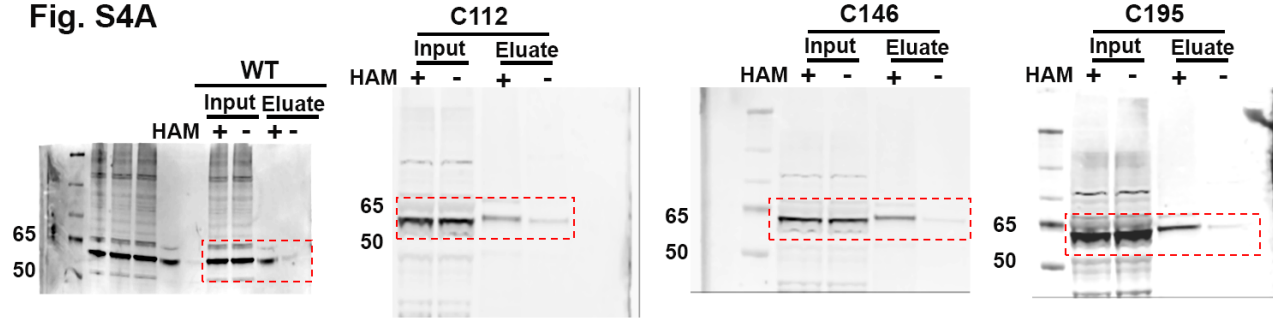


Fig. S4B

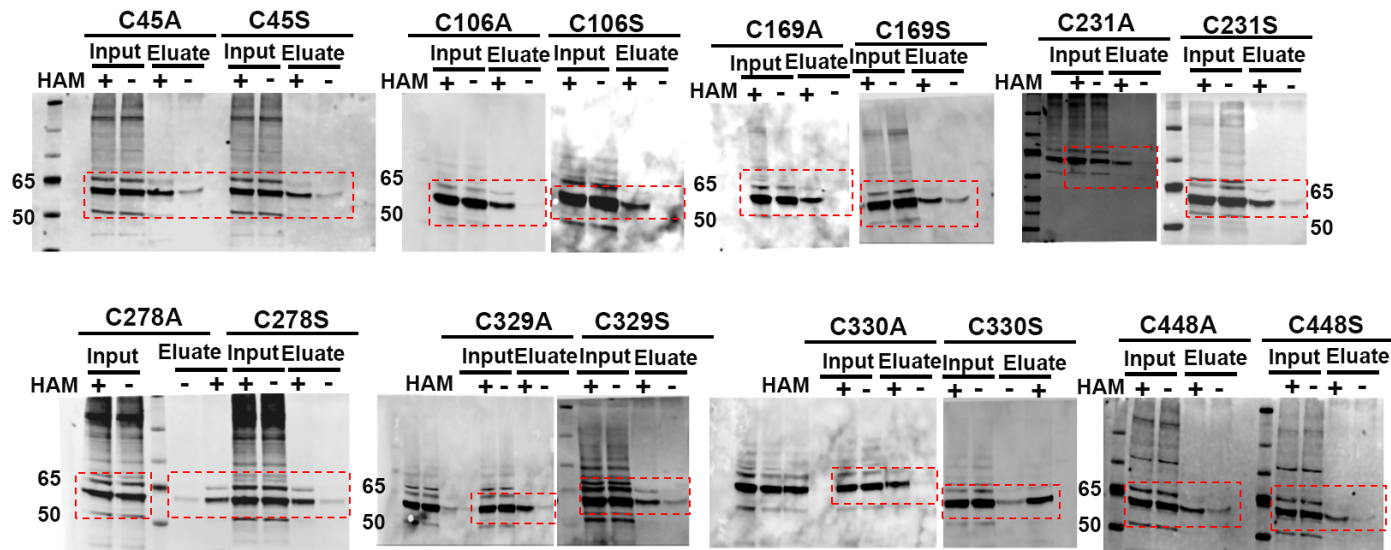


Fig. S4C

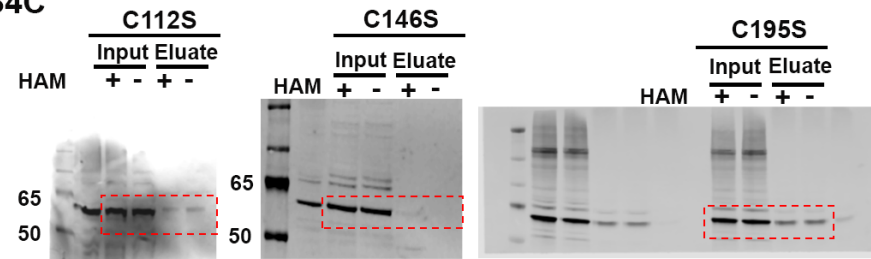


Fig. S8

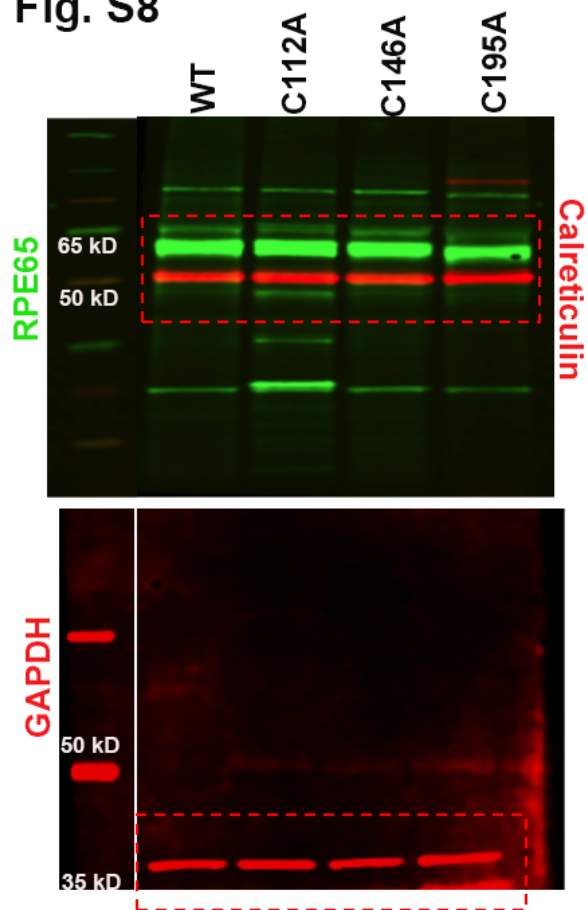


Fig.S9

